Optik 124 (2013) 1049–1052

Contents lists available at SciVerse ScienceDirect

Optik

journal homepage: www.elsevier.de/ijleo

Theoretical study of stimulated Brillouin scattering in high-power dual-clad fiber lasers

Hening Yang, Kailiang Duan*, Baoyin Zhao, Entao Zhang

State Key Laboratory of Transient Optics and Photonics, Xi'an Institute of Optics and Precision Mechanics, Chinese Academy of Science, Xi'an 710119, China

ARTICLE INFO

Article history:
Received 3 August 2012
Accepted 5 January 2013

Keywords:
Stimulated Brillouin scattering
Fiber lasers
Ytterbium
Stokes wave

ABSTRACT

A theoretical analysis of stimulated Brillouin scattering (SBS) in linear cavity Yb^{3+} doped dual-clad fiber lasers is presented by solving the steady-state rate equations with SBS included. Solutions to suppress the detrimental effect in the fiber laser are discussed. It is shown that the first-order Stokes initiated by forward and backward pump light changes exponentially along the fiber, and laser power reduces greatly in the presence of SBS under bidirectional end pump. Furthermore, it is found that the SBS threshold power can be improved effectively by using large mode area fiber and shortening the cavity length.

1. Introduction

High-power, single frequency fiber lasers have many applications in medicine, military, industry, etc. due to high efficiency, compactness, outstanding beam quality and simplified thermal management requirements compared to traditional lasers. However, the maximum power of a CW single frequency fiber laser is limited by thermal effects and nonlinear processes including stimulated Brillouin scattering (SBS), stimulated Raman scattering (SRS), etc. The temperature distribution in the fiber which is in operation has been derived by solving the heat conduction equation [1–4]. Nonlinear effects play an important role in high power fiber lasers. They are induced by the large amount of power density in the small area fiber core. Wang et al. have systematically investigated SRS characteristics in kilowatt ytterbium-doped dual-clad (YDDC) fiber lasers and found solutions to suppress detrimental SRS [4,5]. Numerous publications have studied Brillouin gain spectrum and threshold characterization, besides, several schemes for suppression of SBS in high power fiber amplifiers or lasers have been proposed [6–16], however, systematic investigation of SBS in high-power fiber lasers has not been done yet, as far as we know.

In this paper, we present theoretical study on SBS generated during high power operation of a single-frequency ytterbium doped fiber laser. SBS characteristics have been investigated by numerically solving the differential equations for pump, signal, and Stokes power and the rate equation for the population inversion.

2. Theoretical model

SBS threshold (SBST) is an important parameter described the Brillouin character, and it is defined as the input pump power at which the Stokes power becomes equal to the pump power at the fiber output [14]. Once the input power exceeds the SBST, most of the power is transferred to the backscattered Stokes light which will limit the transmitted laser power, and the Stokes power begins to increase significantly [17]. It is difficult to ascertain the threshold, especially in the presence of gain. There have been only a few published results for SBST in continuous-wave fibers. Generally, SBST under the assumption of no pump depletion is calculated based on Smith's model [6]. However, the threshold level predicted by the model is only an approximate value as the effective Brillouin gain can be reduced by many factors in practice.

The configuration of an end pumped fiber laser oscillator is schematically shown in Fig. 1, in which the amplifying medium has a length of L and a uniform dopant concentration in the fiber core. Coiled fibers have been used to eliminate higher-order modes. $R1$ and $R2$ are the reflectivities of the input mirror and output coupler, respectively. Input mirror is a high-reflectivity mirror which can be either a dichroic mirror or a fiber grating and Output coupler can be either a cleaved fiber facet or a fiber grating. If resonator mirrors are Bragg grating, linewidth of lasers can be less than 0.1 nm or narrower, whereas resonator mirrors are lens or cleaved fiber facet, it may be larger.

The numerical model that uses well-known steady-state rate equations combining with SBS is given by [11]

$$\frac{dP_p^{\pm}(z)}{dz} = \pm\Gamma_p[(\sigma_{ap}+\sigma_{ep})N_2(z) - \sigma_{ap}N]P_p^{\pm}(z) \mp \alpha_p P_p^{\pm}(z) \quad (1)$$

* Corresponding author. Tel.: +86 29 88887613 8042; fax: +86 29 88887603.
E-mail address: kl.duan@163.com (K. Duan).

0030-4026/$ – see front matter © 2013 Elsevier GmbH. All rights reserved.
http://dx.doi.org/10.1016/j.ijleo.2013.01.010

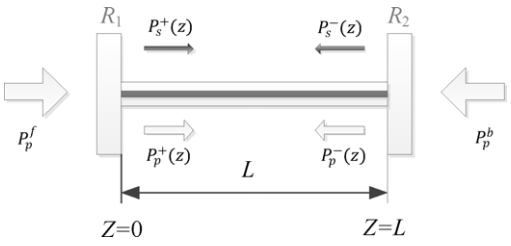

Fig. 1. Schematic configuration of YDDC fiber laser under bidirectional end pump.

$$\frac{dP_s^{\pm}(z)}{dz} = \pm\Gamma_s[(\sigma_{as}+\sigma_{es})N_2(z) - \sigma_{as}N]P_s^{\pm}(z) \mp \alpha_s P_s^{\pm}(z) \mp \frac{g_B}{A_{eff}}P_B^{\pm}(z)P_s^{\pm}(z) \quad (2)$$

$$\frac{dP_B^{\pm}(z)}{dz} = \mp\alpha_B P_B^{\pm}(z) \pm \frac{g_B}{A_{eff}}P_s^{\mp}(z)P_B^{\pm}(z) \quad (3)$$

$$\frac{N_2(z)}{N} = \frac{\frac{[P_p^+(z)+P_p^-(z)](\sigma_{ap}\Gamma_p}{h\nu_p A} + \frac{[P_s^+(z)+P_s^-(z)]\sigma_{as}\Gamma_s}{h\nu_s A}}{\frac{[P_p^+(z)+P_p^-(z)](\sigma_{ap}+\sigma_{ep})\Gamma_p}{h\nu_p A} + \frac{1}{\tau} + \frac{[P_s^+(z)+P_s^-(z)](\sigma_{as}+\sigma_{es})\Gamma_s}{h\nu_s A}} \quad (4)$$

where $p_p^{\pm}$ is the pump power, $p_s^{\pm}$ is the signal power, and $p_B^{\pm}$ is the first-order Brillouin Stokes power (the upper index indicates direction of propagation). z is the location along the fiber, σ_{ap}, σ_{ep}, σ_{as}, σ_{es} are the absorption and emission cross sections (lower index p and s represent the pump light and laser, respectively). N is the number density of the rare earth dopant ions in the core with a doped area A and the ion population density in the upper level is N_2, Γ_p and Γ_s are the power filling factors of the guided mode with the Yb^{3+} distribution. α_p, α_s and α_B represent scattering loss coefficients of pump light, laser and Stokes waves. Generally, the loss coefficients of the Brillouin waves (α_B) are replaced by the laser loss coefficient (α_s) due to the SBS is less than 0.2 nm away from the laser wavelength resulting in negligible difference in the losses between the SBS and the laser [9]. ν_p is the pump frequency, ν_s is the laser frequency and τ is spontaneous lifetime. c is the light velocity in the vacuum, h is the Planck's constant. g_B is the SBS gain which is dependent on linewidth. On the basis of literature [18], the SBS gain decreases with the laser linewidth increases according to

$$g_B = g_0\frac{1}{1+\Delta\nu_s/\Delta\nu_B} \quad (5)$$

where g_0 is the maximum gain and is of the order of 5×10^{-11} m/w, $\Delta\nu_B$ is the intrinsic linewidth of the Brillouin process and is about 50 MHz.

Two-point boundary conditions matched with the above ordinary differential equations can be described as

$$P_s^+(0) = R_1P_s^-(0) \quad (6)$$

$$P_s^-(L) = R_2P_s^+(L) \quad (7)$$

$$P_B^+(0) = R_{1B}P_B^-(0) \quad (8)$$

$$P_B^-(L) = R_{2B}P_B^+(L) \quad (9)$$

where R_1, R_2, R_{1B} and R_{2B} are the reflectivities of the laser and Stokes wavelength at the input ($z=0$) and output ($z=L$) ends, respectively. The laser and Stokes powers are obtained by numerically solving the coupled differential equations (1)–(4).

$$P_s^{out} = (1-R_2)P_s^+(L) \quad (10)$$

$$P_B^- = P_B^-(0) \quad (11)$$

$$P_B^+ = P_B^+(L) \quad (12)$$

3. Simulation results and discussion

The parameters used in the simulation are [11] $\lambda_p = 975$ nm, $\lambda_s = 1082.8$ nm, $R_1 = 0.99$, $R_2 = 0.04$, $R_{1B} = 0.04$, $R_{2B} = 0.04$, $\alpha_p = 3.0\times10^{-3}$ m^{-1}, $\alpha_s = 5.0\times10^{-3}$ m^{-1}, $L = 40$ m, $N = 6\times10^{25}$ m^{-3}, $\sigma_{ap} = 2\times10^{-24}$ m^2, $\sigma_{ep} = 2\times10^{-24}$ m^2, $\sigma_{as} = 3.1\times10^{-27}$ m^2, $\sigma_{es} = 4.2\times10^{-25}$ m^2, $\tau = 0.8$ ms, $\Gamma_s = 0.85$, $\Gamma_p = 0.0012$, $\Delta\nu_s = 10$ GHz, core diameter of Yb^{3+} doped fiber $D_c = 20$ μm and $NA = 0.05$. We have adopted bidirectional end pump in the following calculations.

Fig. 2 shows powers of pump, laser and Stokes waves versus the location along the fiber at different pump power. It is easy to see that pump power decays exponentially whether forward or backward pump power. The backward Stokes wave initiated by forward pump light near $z = L$ undergoes modest gain until it reaches the middle of the fiber. After passing through the region of high gain, it reaches an appreciable power level and changes exponentially along the fiber. The changing process of forward Stokes wave initiated by the backward pump light near $z = 0$ is the same as the backward Stokes wave. The difference between them is that the forward Stokes power is smaller than backward Stokes power, which is because of the reflectivity of the resonator mirrors. Stokes waves do not emerge until pump power is about 400 W in calculation. Because of the large first-order Stokes, the laser undergoes strong attenuation in the first half of the fiber and increases rapidly after approximately 20 m. It can be seen that distribution of laser power (forward propagating) along the fiber changes obvious after presence of Stokes. It is obvious that the increase of laser power becomes slower, even emerges negative growth before the middle of the fiber with the increase of pump power by contrasting the four pictures in Fig. 2, which is because the Stokes steals the population inversion and makes the laser less able to compete for the gain. Besides, Stokes receives much power from the laser and growths rapidly after reaching the SBS threshold.

The distribution character of population inversion along the fiber changes a lot with the increase of pump power in Fig. 3. The population inversion at $z = 0$ decreases gradually whereas it increases at $z = L$ and at the middle of the fiber when the total pump power becomes large. This is because there is an extra strong saturation of population inversion by the odd-order Stokes waves at the front end, whereas it does not happen at the back end and middle of the fiber. Meanwhile, the depletion of population inversion by output power tails off because the increase of laser power gets

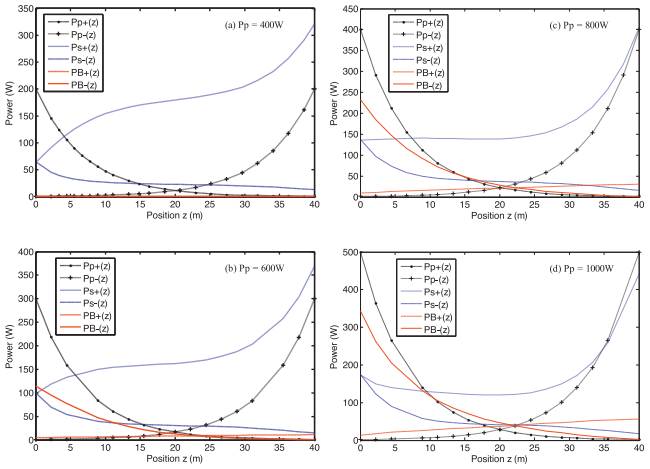

Fig. 2. Pump, laser and Stokes powers versus the location along the fiber for different pump powers. $p_p^+(z)$, $p_s^+(z)$, $p_B^+(z)$: pump, laser and Stokes powers of forward propagating, $p_p^-(z)$, $p_s^-(z)$, $p_B^-(z)$: pump, laser and Stokes powers of backward propagating.